



**ARTICLE**

# Morphological Evaluation of PLA/Soybean Oil Epoxidized Acrylate Three-Dimensional Scaffold in Bone Tissue Engineering

Mahmood Hameed Majeed\* and Nabeel Kadhem Abd Alsaheb

Department of Biomedical Engineering, Al Nahrain University, Al Jadriya Bridge, Baghdad, 64074, Iraq

\*Corresponding Author: Mahmood Hameed Majeed. Email: mahmoodhameedmajeed@gmail.com; st.mahmood.hameed@ced.nahrainuniv.edu.iq

Received: 22 October 2021 Accepted: 14 January 2022

## ABSTRACT

Tissue engineering's main goal is to regenerate or replace tissues or organs that have been destroyed by disease, injury, or congenital disabilities. Tissue engineering now uses artificial supporting structures called scaffolds to restore damaged tissues and organs. These are utilized to attach the right cells and then grow them. Rapid prototyping appears to be the most promising technology due to its high level of precision and control. Bone tissue replacement "scaffolding" is a common theme discussed in this article. The fused deposition technique was used to construct our scaffold, and a polymer called polylactic acids and soybean oil resin were used to construct our samples. The samples were then divided into two groups; the first group was left without immersion in the simulated body fluid and served as a control for comparison. The second group was immersed in the simulated body fluid. The results of the Field Emission Scanning Electron Microscope (FESEM), Energy Dispersive X-ray Spectroscopy (EDX) and X-ray diffraction (XRD) were utilized to interpret the surface attachment to ions, elements, and compounds, giving us a new perspective on scaffold architecture. In this study, an innovative method has been used to print therapeutic scaffold that combines fused deposition three-dimensional printing with ultraviolet curing to create a high-quality biodegradable polymeric scaffold. Finally, the results demonstrate that adding soybean oil resin to the PLA increased ion attachment to the surface while also attracting tricalcium phosphate formation on the surface of the scaffold, which is highly promising in bone tissue replacement. In conclusion, the soybean oil resin, which is new in the field of bone tissue engineering, shows magnificent characteristics and is a good replacement biopolymer that replaces many ceramic and polymeric materials used in this field that have poor morphological characteristics.

## KEYWORDS

Bone tissue engineering; polylactic acid; soybean oil; biodegradable polymers; fused deposition modeling; scaffold

## 1 Introduction

In recent years, the scientific community has focused on developing more environmentally friendly alternatives to conventional oil-based molecules [1]. Tissue engineering, in turn, enables scientists to produce biocompatible materials for use in the preservation, restoration, or improvement of bones, tissues, or organs. Because of the tissue engineering needs, a new scaffold is needed to supply a temporary artificial matrix for cell seeding. Porosity, biocompatibility, biodegradability: Scaffolds must



have all three of these characteristics [2–4]. While *in-vitro* or *in-vivo* regenerative therapy might generate stresses and loadings, the scaffold must sustain those to retain their magnitude during *in-vitro* or *in-vivo* regenerative therapy. To overcome this, more work to be done to construct scaffolds without the immune system rejecting them. Furthermore, the scaffolds should keep the porosity structure in place to maintain cellular growth conditions [5,6]. When building complex porous structures, frameworks or tuning their distribution, there is still a challenge in creating precise structures [7].

Currently, tissue engineering utilizes artificial scaffolds to nurture tissue and organ development. Pre-defined forms are used to build scaffolds that are then filled with a porous material. External geometry, porosity, porous interconnectivity, individual pore size, and surface area are part of their structural qualities. An artificial scaffold is particularly utilized to promote bone, cartilage, ligaments, skin, blood vessels, nerves, and muscle growth [8,9].

The term “additive manufacturing” or “3D printing” refers to a manufacturing procedure of layering materials to build 3D-model items instead of subtractive manufacturing methodologies [1]. A diverse array of materials, including polymers, ceramics, metals, and composites, may be fabricated with 3D printing using a wide range of bespoke forms and densely packed or macro-or micro-porous architectures [10–13].

The most prevalent polymers are also known as PGA, PLA, and the copolymers of these, the copolymers of poly(lactic-co-glycolic acid) (PLGA). Poly(lactic acid) (PLA), poly(glycolic acid) (PGA), and poly(lactic/polyglycolic acid) copolymers all suffer from deterioration due to random hydrolysis of their ester linkages. PLA has the ability to decompose to lactic acid when it becomes attached to human body fluid; also, lactic acid is normally found in human body as chemical byproduct of anaerobic respiration. Both synthetic and natural materials can be used to make scaffolds [5].

Biological and triglyceride structures, especially plant oils, make them a suitable alternative for manufacturing bio-based UV-curable polymers. Although most oil-based resins reported often have low mechanical qualities and heat resistance, limiting their applicability to petroleum resins, these traits are not inherent to oil-based resins and can be overcome. Since this is the case, a large number of experiments have been undertaken to improve qualities for plant oil-based resins [14–16]. Current research focuses on using engineered scaffolds with pre-designed shapes, structures, and functions for improved tissue regeneration. Tissue engineering scaffolds, in which the 3D printed macro-micro structure morphologically mimics the multi-scale structure of actual body tissues, are favorable when 3D printing is employed [17–20].

The purpose of this research is to create a three-dimensional scaffold that may be utilized to replace a damaged part of biological tissue while also acting as an ECM (extracellular matrix) that promotes tissue repair and regeneration. The paper used a basic comparison of PLA and PLA with soybean oil resin to determine which design is optimal for attracting more components that aid in bone repair and regeneration. A variety of chemical and morphological experiments are used to evaluate the effect of adding soybean oil resin on the adsorption enhancement of ions, elements, and compounds on the scaffold.

## 2 Materials and Methods

### 2.1 Materials (Poly(lactic Acid) and Soybean Oil Epoxidized Acrylate)

Poly(lactic acid) is one of the most extensively used synthetic polymers for medical products, barrier membranes, regenerative treatments in dentistry, orthopedics, sutures, tissue stents, and scaffolds are derived from lactic acid [21,22].

There is a non-enzymatic degradative disruption of the enclosed ester bonds during PLA degradation. In the autocatalytic reaction, CO<sub>2</sub> and H<sub>2</sub>O are eliminated as the last products. Due to the cleavage of ester bonds, PLA's formation of lactic acid (which causes the surrounding environment to go sour) is one of the major issues [2,23,24]. The PLA used in our study is listed in has a brand name MKK, Diameter 1.75 millimeters, and the country of origin is China.

Ring-opening reaction of epoxidized plant oils yields epoxy acrylate plant oil (EA). Many EA oil-based resins have limited mechanical and heat resistance qualities, making them less applicable to petroleum resins. A major advantage of soybean oil is that it may replace petroleum-based chemicals with bio-based alternatives [25]. In our research, the soybean oil resin purchase from Shenzhen any cubic technology company, as well as the curing device model anycubic, wash and cure version two.

## 2.2 Three Dimensional Printing

Fused deposition modeling (FDM), also known as fused filament manufacturing, is a three-dimensional printing technology; in FDM, a heated extrusion head guides a filament to deposit molten polymer on a bed where the part is printed [16]. Special processability is also necessary for FDM procedures, along with filament generation and layer deposition. Extruded material needs to have a low melting temperature and a quick solidification time [16,17]. In addition, the adhesion between layers and the uniform distribution of all additives are important for the printability and strength of printed objects. The intricate nature of FDM 3D printing adds to the already complicated printing parameters [18]. The types of polymers that are amenable to printing with FDM include acrylonitrile butadiene (ABS), polycarbonate (PC), and poly (lactic) acid (PLA). The three other polymers (cellulose, starch, and vegetable oil) are not biodegradable, and PLA is, by far, the most commonly tested polymer for 3D printing from the limited number of biodegradable polymers. To date, however, in many applications, particularly in industrial settings, the material has been prevented from acting in this manner due to its poor mechanical properties [26–29]. Some isolates contained in PLA have a compound that prevents them from being used in conducting components [1,2,30]. In order to meet each of these problems, various additives were added to PLA to enhance its strength and conductivity. This research used PLA/soybean oil resin to discover the additives that increase the bioactivity function of PLA/soybean oil resin while preserving its biodegradability. Soybean oil increases the migration and growth of cells, in particular bone cells, so these experiments demonstrate this possibility.

In this article, a new novel method has been used by combining the traditional three-dimensional printing method, which is fused deposition modeling, and UV resin three-dimensional printing. The sample is first printed with an FDM printer, and then the resin is injected into the samples. Finally, the samples are exposed to UV light to get the resin hardened. While researchers in this field used only one of the previously mentioned methods, either FDM or resin three-dimensional printing, to print their scaffold, Also, using soybean oil as a biodegradable polymer is new in the field of bone tissue engineering. The research seeks to find alternative replacements for the ceramic materials that have been widely used in the bone tissue engineering field and replace them with biopolymers.

To summarize, in our studies, the FDM used was found to be the trustworthiness is Creality ender 3 model. The printing method involved using our 3D printer to create the scaffold. The nozzle head, which determines the print's diameter, was selected with a nozzle diameter of 0.3 mm. The cube's dimensions are 10 mm × 10 mm × 10 mm, which is divided into layers of 10 circular bars. The thickness of the next layer is 0.5 mm, and it is a circular bar, as shown in Fig. 1.

The design is printed in the program called SolidWorks; after printing the scaffold structure, the structure is filled with soybean oil resin, and then it enters a curing process that utilizes anycubic curing device two from Shenzhen Company Ltd, China. UV radiation at a wavelength of 405 nm was used exposure time is 30 min for each sample. Not all the porosity are filled during this procedure to insure the transport of nutrients and other bodily fluid during defected bone regeneration the PLA scaffold are design to have 50% porosity according to design sheet as shown in Fig. 1; the 0.5 ml of soybean injected after that will not fill all the porosity due to the ability of PLA to absorb some of the fluid during injection so this can be seen on the change of the color of PLA scaffold after injected by soybean oil resin as shown in Fig. 2; also soybean oil resin has ability to degrade faster than PLA it give the opportunity to open passage during bone healing for transport nutrient.

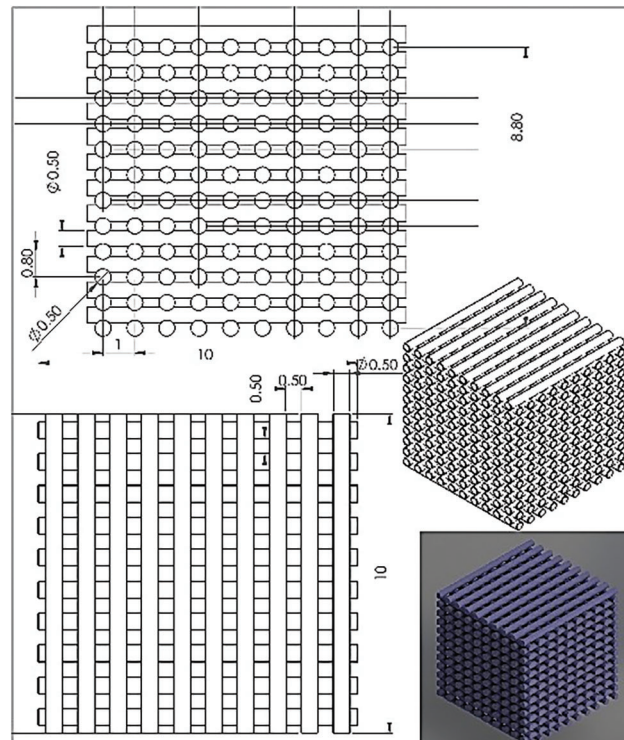


**Figure 1:** Shows the cubic scaffold's design sheet in SolidWorks, all dimensions in millimetres

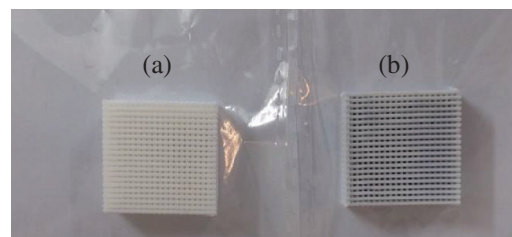


**Figure 2:** (a) Shows sample material used PLA only and printed using 3D printer. (b) Shows sample material used PLA and printed using 3D printer and then injected with 0.5 ml of soybean oil

### 2.3 Simulated Body Fluid (In Vitro Bioactivity Evaluation)

A simulated bodily fluid (SBF) containing 1.5 times the concentration of ions in human blood plasma was utilized to test the apatite mineralization capability of the scaffolds in our study. This solution was produced, and the sample concentration as shown in Table 1, in accordance with the methods provided by [1]. For 28 days, 1 cm \* 1 cm samples were submerged in 250 mL of SBF (pH 7.4) in an incubator at 37°C. In all samples, the SBF fluid was replaced on a weekly basis. The samples were washed with deionized water and dried in a 70 Celsius hot air oven at the end of the time period. The SBF was used to immerse two samples. All of the chemical reagents used in our research were purchased from (Sigma-Aldrich). The work was done in the Materials Research Department of the Ministry of Science and Technology in Baghdad, Iraq.

Bioreactivity assessments, which include testing for bone bonding with implant materials, are usually performed using *in vivo* animal testing, which began with a dog study performed by Dr. Levert in 1829. Because of the fibrous connective tissue between the implant and the bone, these artificial materials,

including steel, Co–Cr alloy, alumina, and titanium, were never released into the surrounding bone tissue; This was a normal defense mechanism employed by the living body in the face of potential external invaders. According to Hench and his colleagues, in 1972, the first synthetic material that became attached to bone without any fibrous tissue was a glass compound composed of  $\text{Na}_2\text{O}$ ,  $\text{CaO}$ ,  $\text{SiO}_2$ , and  $\text{P}_2\text{O}_5$  [31–36].

**Table 1:** The SBF elements standard was used in our experiment

Item	Description	Quantity (g) in 1000 (ml)
1	Sodium chloride ( $\text{NaCl}$ )	8.036
2	Potassium chloride ( $\text{KCl}$ )	0.225
3	Calcium chloride ( $\text{CaCl}_2$ )	0.293
4	Sodium bicarbonate ( $\text{NaHCO}_3$ )	0.352
5	Potassium hydrogen phosphate ( $\text{K}_2\text{HPO}_4$ )	0.230
6	Magnesium chloride, 6-Hydrate ( $\text{MgCl}_2 \cdot 6\text{H}_2\text{O}$ )	0.311
7	Sodium sulphate ( $\text{Na}_2\text{SO}_4$ )	0.072

Every single time that an interface between bone and bioactive materials (apatite layers) was explored, it was revealed that there were layers of apatite [31].

In the present biomaterials field, the use of SBF for immersion investigations is commonly regarded as a reliable method for assessing bioactivity. Accordingly, these are valid only if the appropriate testing parameters are set for each biomaterial type; for example, the SBF volume should be consistent across a wide range of objects, big particles, porous objects [25,31].

Within a matter of weeks after discovering the SBF method, material scientists embraced the method as an in vitro indication of bone-bonding potential; This was fixed in 1991 when the original SBF had insufficient  $\text{SO}_4^{+2}$  ions that are found in human blood plasma. Even after correcting for the effects of differing amounts of chloride and bicarbonate ions, the corrected SBF is still richer in chloride ions and poorer in bicarbonate ions than human blood plasma. Correcting the gap between males and females has been studied more closely between 2003 and 2004 [18–20]. After considering the material's stability and reproducibility of the apatite formation, the improved SBF was submitted to the ISO/TC150 of the International Organization for Standardization for approval (ISO). Apatite-forming implant materials were standardized in 2007 when the SBF was officially certified as ISO 23317 [31,37–40].

Many experiments demonstrate that some bioactive materials do create stable chemical bonds with the bone. To answer this question, the first statement reads: “Is the testing for SBF in vitro the most suited way to assess the bioactivity of materials?” If the overall purpose is to encourage bone repair, the answer is “Yes”. Contrary to that assertion, if the application is intended to be in contact with soft tissues, then SBF tests may have different results or maybe have no results at all; in this case, the apatite-forming capability could lead to soft tissue calcification. As another example, it has been estimated that a skin wound's natural healing process takes between 14 and 21 days after the harm has occurred [1,23,41,42].

#### **2.4 Field Emission Scanning Electron Microscope (FESEM) and Energy Dispersive X-Ray Spectroscopy (EDX) Study**

The SEM examination was carried out to identify the morphological analysis of the sample with or without SBF solution and demonstrate the PLA polymer bioactivity with and without soybean injection. The EDX analysis was used to determine and analyze the chemical, elemental, and particle distribution compared to the groups that were not immersed [2,4,43–45].

Following sample preparation, each sample was sputtered with gold, and the micro-morphological SEM analysis for each specimen was performed at increasing magnifications. The samples are analyzed at Tehran University/Iran using a device called MIRA3 TESCAN.

### 2.5 Fourier-Transform Infrared Spectroscopy (FTIR)

The Fourier Transform Infrared (FTIR) technique was created to simultaneously determine organic components, including chemical bonds and organic content (e.g., protein, carbohydrate, and lipid). For researchers, Fourier transforms infrared (FTIR) is a critical analytical tool. This technique is useful for determining the properties of liquids, solutions, pastes, powders, films, fibers, and gases. Additionally, this analysis can be used to examine substances on the surfaces of substrates [45,46]. FTIR is highly popular in comparison to other forms of characterization analysis. This characterization analysis is relatively quick, accurate, and sensitive [46]. FTIR analysis involves exposing samples to infrared (IR) radiation. The IR radiations then affect the atomic vibrations of a molecule in the sample, resulting in the energy being absorbed and/or transmitted in a specific manner. This enables the FTIR to determine the exact molecular vibrations present in a sample [1,29,46].

## 3 Results and Discussion

For comparison, the samples were divided into two groups: group A, which did not immerse in SBF fluid and included samples one and two, and group B, which included samples three and four and immersed in SBF. Each group had two samples PLA and PLA, injected with soybean oil resin as shown in Table 2.

**Table 2:** The samples specifications that were used in our study

Sample number	Material types	Design shape	Group	Printing method	Simulated body fluid
1	PLA only	cubic	A	FDM printer	Non immerse
2	PLA and soybean oil resin	cubic	A	FDM printer then injected with soybean oil resin	Non immerse
3	PLA only	cubic	B	FDM printer	immerse
4	PLA and soybean oil resin	cubic	B	FDM printer then injected with soybean oil resin	immerse

### 3.1 Field Emission Scanning Electron Microscopy (FESEM)

According to the FESEM data obtained from control group A samples one and two, when we compare sample one that only contained PLA with the sample two PLA injected with soybean oil resin, we notice the presence of a transparent layer permeate between the pores, which is evidence of the presence of soybean resin. Some of this layer can be seen on the fibre itself due to absorbing some of the soybean oil during injection by the PLA, as shown in Figs. 3 and 4.

When group A sample one was compared to group B sample three, a thin coating of element and mineral precipitated on the surface of sample three due to immersion in SBF solution. These particles included Na, Cl, and K, as well as Gold, which was visible due to the FESEM image preparation processes that included polishing the specimens with it, as shown in Table 3.

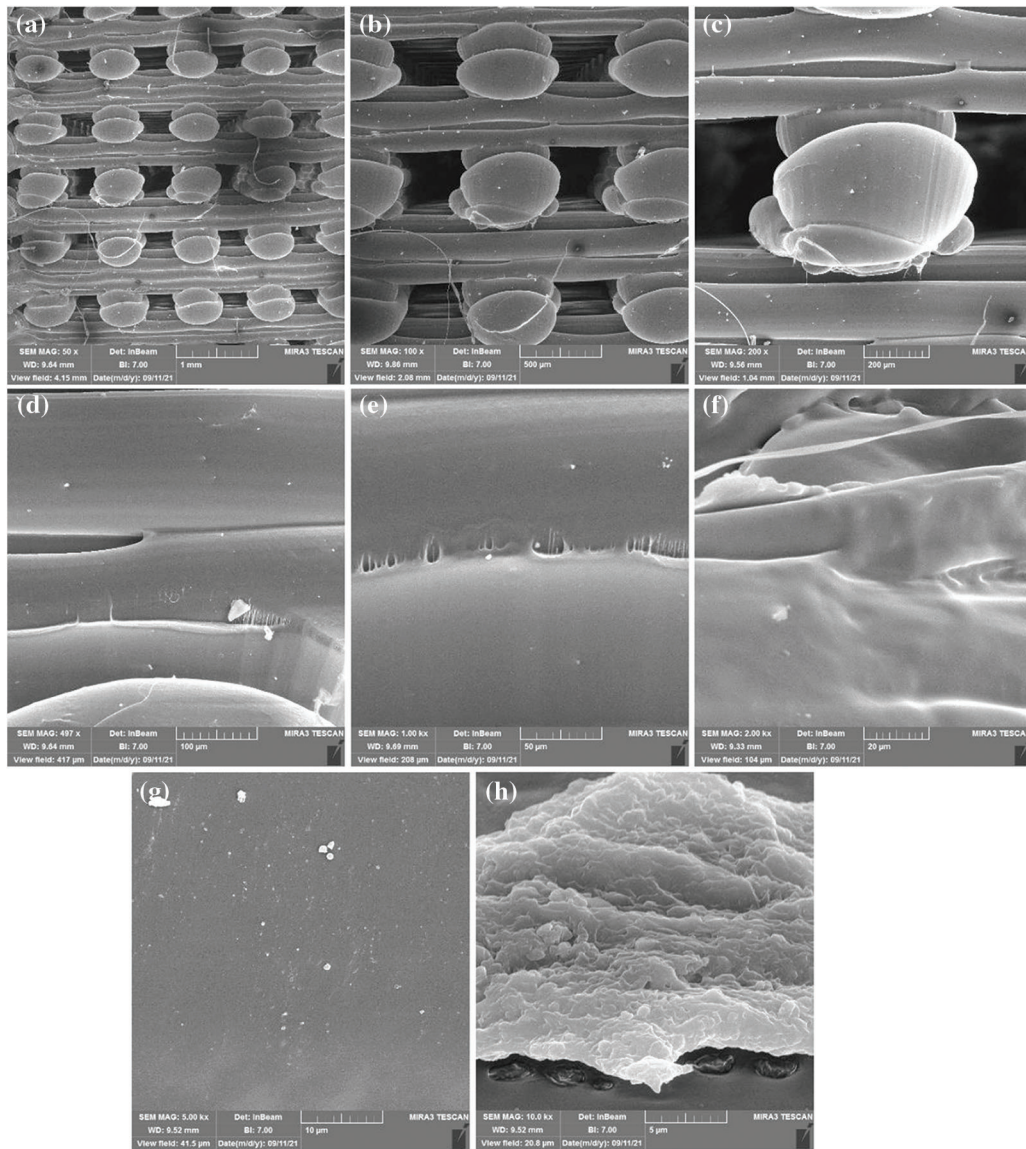


**Figure 3:** Scanning electron microscopy with different magnification levels for sample one made from polylactic acids only in cubic design (a) magnification level 50x and view field 4.15 mm (b) magnification level 100x and view field 2.08 mm (c) magnification level 200x and view field 1.04 mm (d) magnification level 497x and view field 417  $\mu\text{m}$  (e) magnification level 1 Kx and view field 208  $\mu\text{m}$  (f) magnification level 2 Kx and view field 104  $\mu\text{m}$  (g) magnification level 5 Kx and view field 41.5  $\mu\text{m}$  (h) magnification level 10 Kx and view field 20.8  $\mu\text{m}$

By comparing sample two in group A with sample four in group B, a thick layer of minerals and elements can be seen on the sample immersed in SBF fluid due to the high bioactivity of the surface due to injected the sample with soybean oil. That is because soybeans are enriched with isoflavones that have attracted much attention due to their ability to prevent osteoporosis and stimulate bone formation [47,48]. Other researchers, Nayeem et al. [49], investigated how soy isoflavones affect bone mineral density (BMD). Soybean oil offers beneficial health properties such as antiarrhythmic and anti-inflammatory. Further, the significant amount of Vitamin K present in soybean oil plays a pivotal role in bone health A

wide range of interest has focused on the topic of soy and health benefits, especially the role of soy in health promotion and chronic disease prevention and treatment. Various nutritional supplements have been produced from soybeans on the market, such as vitamin E, lecithin, and isoflavones [48].

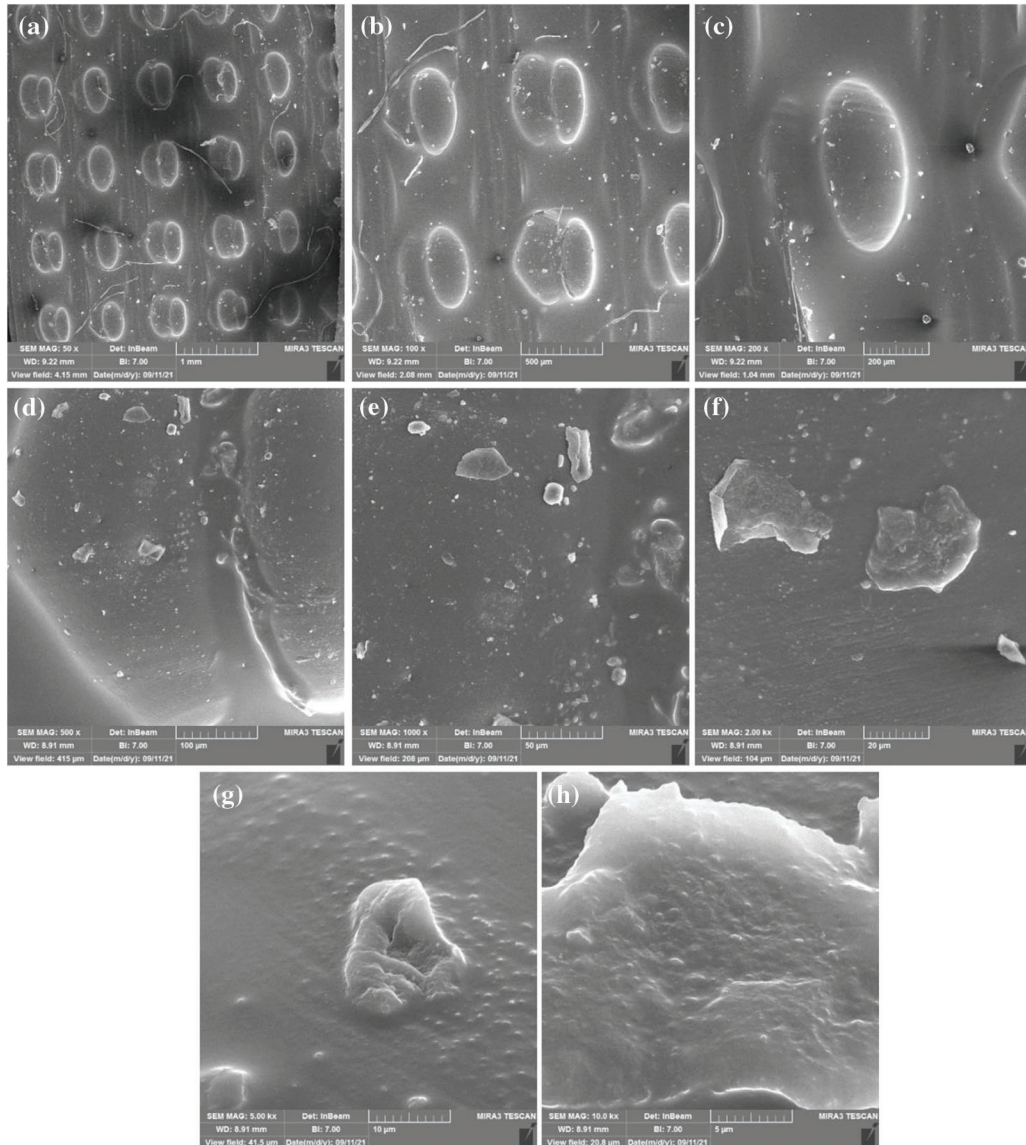


**Figure 4:** Scanning electron microscopy with different magnification levels for sample two that were made from polylactic acids and injected with soybean oil resin in cubic design (a) magnification level 50x and view field 4.15 mm (b) magnification level 100x and view field 2.08 mm (c) magnification level 200x and view field 1.04 mm (d) magnification level 500x and view field 415  $\mu\text{m}$  (e) magnification level 1 Kx and view field 208  $\mu\text{m}$  (f) magnification level 2 Kx and view field 104  $\mu\text{m}$  (g) magnification level 5 Kx and view field 41.5  $\mu\text{m}$  (h) magnification level 10 Kx and view field 20.8  $\mu\text{m}$

If we compare the sample three and four in group B the precipitation in sample four is high and obvious this indicated the bioactivity of soybean oil and formation of tricalcium phosphate that attracted by the bioactivity of the surface from the SBF solution as shown in Figs. 5 and 6.

**Table 3:** Analysis conditions and specification used in EDX for all samples

X-ray analysis	Conditions	Detector	Conditions
Beam current (nA):	10.000	Gold layer ( $\mu\text{m}$ )	20.00
Magnification:	250	Active area ( $\text{mm}^2$ )	10.00
Live time (s):	30	Crystal	Si
Width (keV):	20	Coating thickness (nm)	15.00

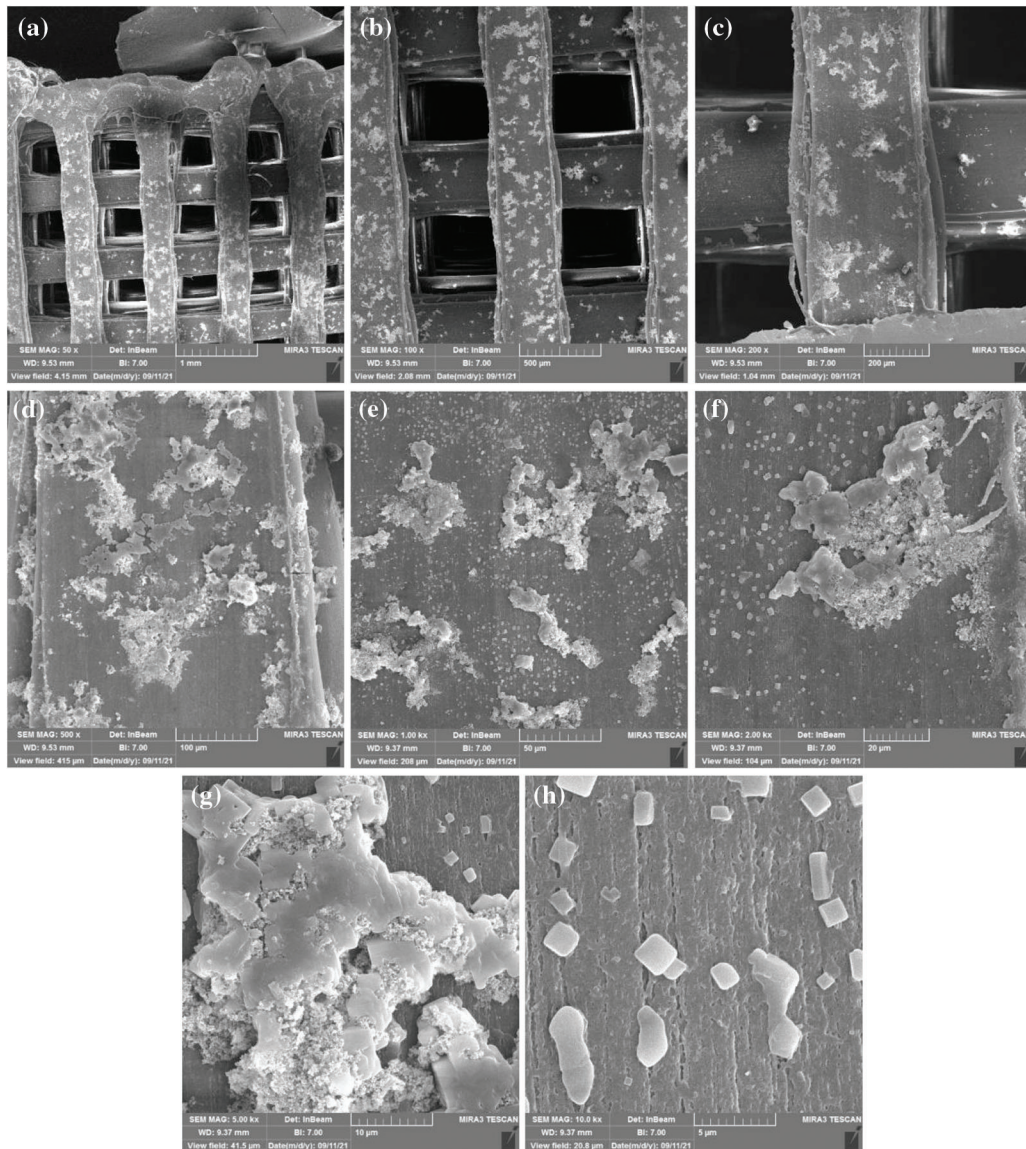


**Figure 5:** Scanning electron microscopy with different magnification levels for sample three that was made from polylactic acids only in cubic design and immerse in SBF solution (a) magnification level 50x and view field 4.15 mm (b) magnification level 100x and view field 2.08 mm (c) magnification level 200x and view field 1.04 mm (d) magnification level 500x and view field 415  $\mu\text{m}$  (e) magnification level 1 Kx and view field 208  $\mu\text{m}$  (f) magnification level 2 Kx and view field 104  $\mu\text{m}$  (g) magnification level 5 Kx and view field 41.5  $\mu\text{m}$  (h) magnification level 10 Kx and view field 20.8  $\mu\text{m}$

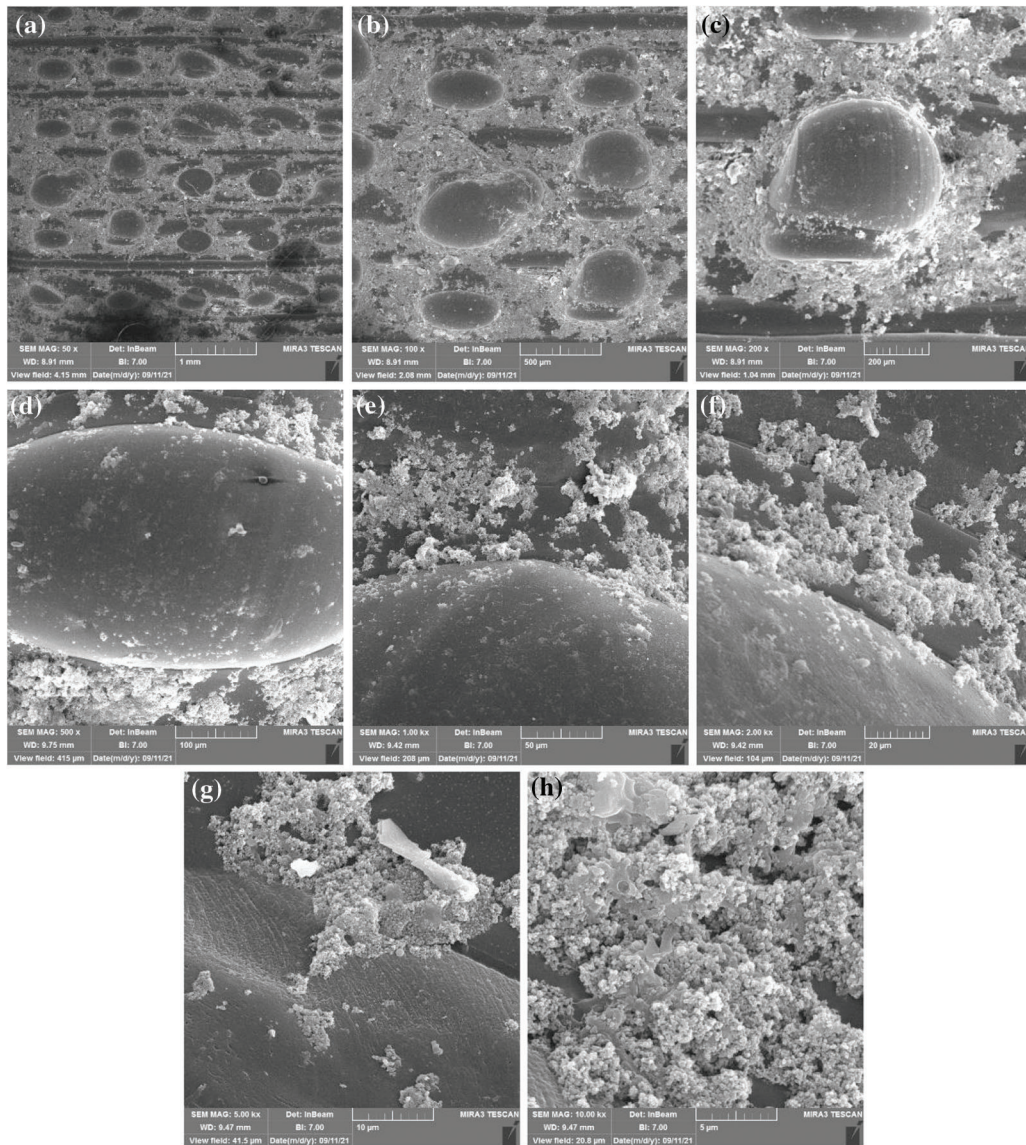


**Figure 6:** Scanning electron microscopy with different magnification levels for sample four that were made from polylactic acids and injected with soybean oil resin in cubic design and immersed in SBF solution (a) magnification level 50x and view field 4.15 mm (b) magnification level 100x and view field 2.08 mm (c) magnification level 200x and view field 1.04 mm (d) magnification level 500x and view field 415  $\mu\text{m}$  (e) magnification level 1 Kx and view field 208  $\mu\text{m}$  (f) magnification level 2 Kx and view field 104  $\mu\text{m}$  (g) magnification level 5 Kx and view field 41.5  $\mu\text{m}$  (h) magnification level 10 Kx and view field 20.8  $\mu\text{m}$

### 3.2 Energy Dispersive X-Ray Spectroscopy Analysis (EDX)

EDX analysis was used to confirm the formation and constituents of samples containing PLA and those containing PLA and soybean oil resin. Different locations were focused throughout that time, as well as the relevant peaks are depicted in Fig. 7. Carbon atoms and oxygen can be seen in spectrum one for sample one, indicating that PLA contains an organic component. As shown in Table 4, the percentages of these elements, and the results reveal that carbon has a higher percentage than oxygen.

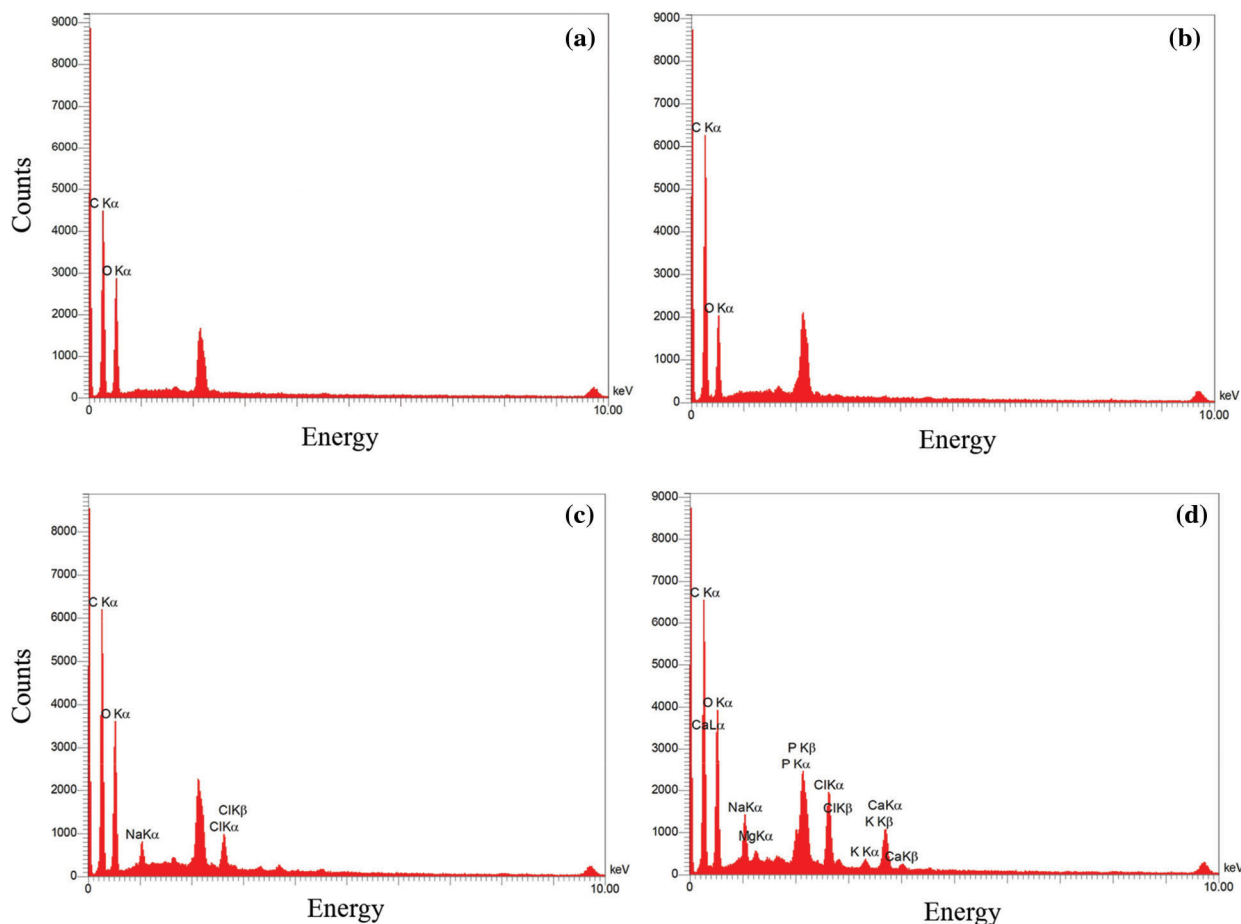


**Figure 7:** EDX data of different samples Y-axis represents counts and X-axis represents energy in (keV) (a) sample one (b) sample two (c) sample three (d) sample four

**Table 4:** EDX quantitative results for all samples

	Element	Line	Intensity	Weight (%)	Atomic (%)
Sample 1					
	C	Ka	443.4	45.31	52.46
	O	Ka	210.4	54.69	47.54
Sample 2					
	C	Ka	637.7	49.05	56.18
	O	Ka	232.1	50.95	43.82
Sample 3					
	C	Ka	595.3	43.89	53.45
	O	Ka	399.6	43.35	39.63
	Na	Ka	123.7	7.39	4.70
	Cl	Ka	193.1	5.37	2.21

(Continued)

Table 4 (continued)					
	Element	Line	Intensity	Weight (%)	Atomic (%)
Sample 4					
	C	Ka	653.9	40.08	52.07
	O	Ka	449.9	36.06	35.17
	Na	Ka	211.2	7.76	5.27
	Mg	Ka	78.8	2.35	1.51
	P	Ka	136.3	2.59	1.30
	Cl	Ka	345.9	6.29	2.77
	K	Ka	62.0	1.14	0.46
	Ca	Ka	202.5	3.71	1.44

In spectrum two, two elements are observed because the sample is composed of two organic materials PLA and soybean oil resin; hydrogen will not occur and detect in the EDX analysis; also, the percentage of carbon is higher in sample two than in sample one.

A new element (Na and Cl) was discovered in spectrum three for sample three immersed in SBF. This new element (Na and Cl) suggested the attachment of the elements from the solution onto the sample's surface.

According to spectrum four and Table 4, a new element (Mg, K, P, Ca) was discovered attached to the surface. Fig. 6 also shows the formation of calcium phosphate on the surface. From the weight percent of calcium and phosphate, which are respectively (3.71, 2.59), the percentage of Ca/P molar ratio can be calculated ( $\text{Ca/P} = 1.432$ ) referred to the reference [37], this number indicated that the structure formed on the sample is tricalcium phosphate.

### 3.3 FTIR Results

FTIR analysis of PLA sample one indicated the ester ( $1748.90$  and  $1180.71 \text{ cm}^{-1}$  for  $-\text{COO}-$  and  $-\text{CO}-$ , respectively) and  $-\text{CH}_3$  (Stretching) group absorption peaks ( $2947.28 \text{ cm}^{-1}$ ). Additionally, an absorption peak associated with  $\text{C}=\text{O}$  stretching ( $1748.90 \text{ cm}^{-1}$ ) was found. Bands corresponding to  $\text{CH}_3$ 's bending vibrations were discovered in the polymer spectra at  $1454.10 \text{ cm}^{-1}$  as higher intensity peaks. All of the peaks are listed as shown in Table 5, for PLA sample one.

**Table 5:** Functional group and corresponding wavenumber for sample one made from polylactic acid

	Functional group	Standard frequency ( $\text{cm}^{-1}$ )	Sample one (PLA only)
1	$-\text{CH}_3(\text{S})$	2850–3000	2947.28
2	$-\text{C}=\text{O}$	1650–1750	1748.90
3	$-\text{C}-\text{O} (\text{COOH})-\text{OH}$	1000–1300	1080.57 1180.71 1270.74
4	$-\text{CH}_3(\text{B})$	1375–1475	1454.10

For PLA injected with soybean oil sample two, the band appears as shown in Fig. 8,  $-\text{CH}_3$  (Stretching) group between ( $2500\text{--}3000 \text{ cm}^{-1}$ ); and the peak appears in ( $1751.13 \text{ cm}^{-1}$ ) in the double bond area between

(1500–2000  $\text{cm}^{-1}$ ), indicating an active carbonyl group. A significant signal (1040.76, 1081.07, 1126.66, and 1179.97  $\text{cm}^{-1}$ ) was detected in the fingerprint region, indicating the presence of a vinyl-related molecule.

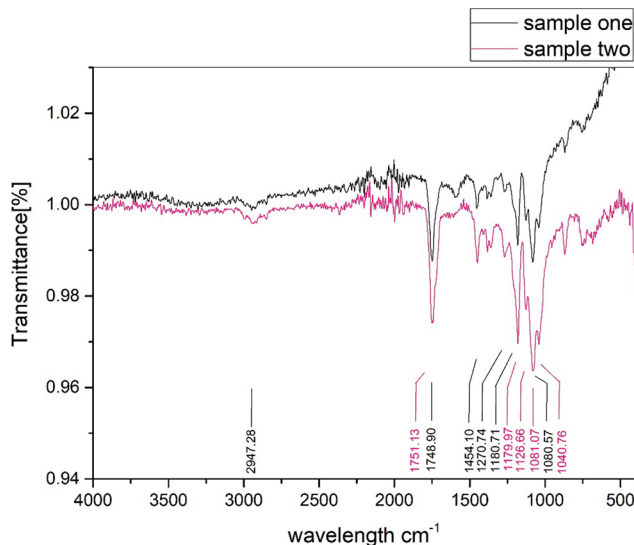


**Figure 8:** Shows the FTIR spectrum of polylactic acids (sample one) and the FTIR spectrum of polylactic acids injected with soybean oil resin (sample two) obtained from Bruker device at the Materials Research Department of the Ministry of Science and Technology in Baghdad, Iraq

### 3.4 XRD Results

XRD measurements are made at an angle of 10–80°, and a scanning rate of 5 °/min using a Shimadzu XRD–6000 X-ray Diffractometer (LabX version) equipped with CuK radiation (1.5406Å) operated at 30 mA and 40 keV. Origin Pro software was used to plot the X-ray data.

The X-ray diffraction (XRD) technique was used to investigate the phase purity, and crystallinity of pure PLA and PLA injected with soybean oil resin, as shown in Fig. 9. All the XRD patterns reflected the existence of pure PLA peaks and showed intensity with a broad maximum appearing at approximately  $2\theta \sim 16.5^\circ$ , which confirmed that the PLA had no polymorphic crystalline transition [50]. However, new peaks emerged in the immersed PLA/soybean oil architecture sample four, indicating the presence of hydroxyapatite elements as shown in Table 6. A new peak was observed at  $2\theta \sim 31.8315^\circ$  as compared with the commercial hydroxyapatite peak and the peak obtained by Kien et al. [51]. This occurs only with the soybean oil resin-treated sample and demonstrates the attraction of hydroxyapatite with the soybean-treated sample, as shown in Fig. 9d.

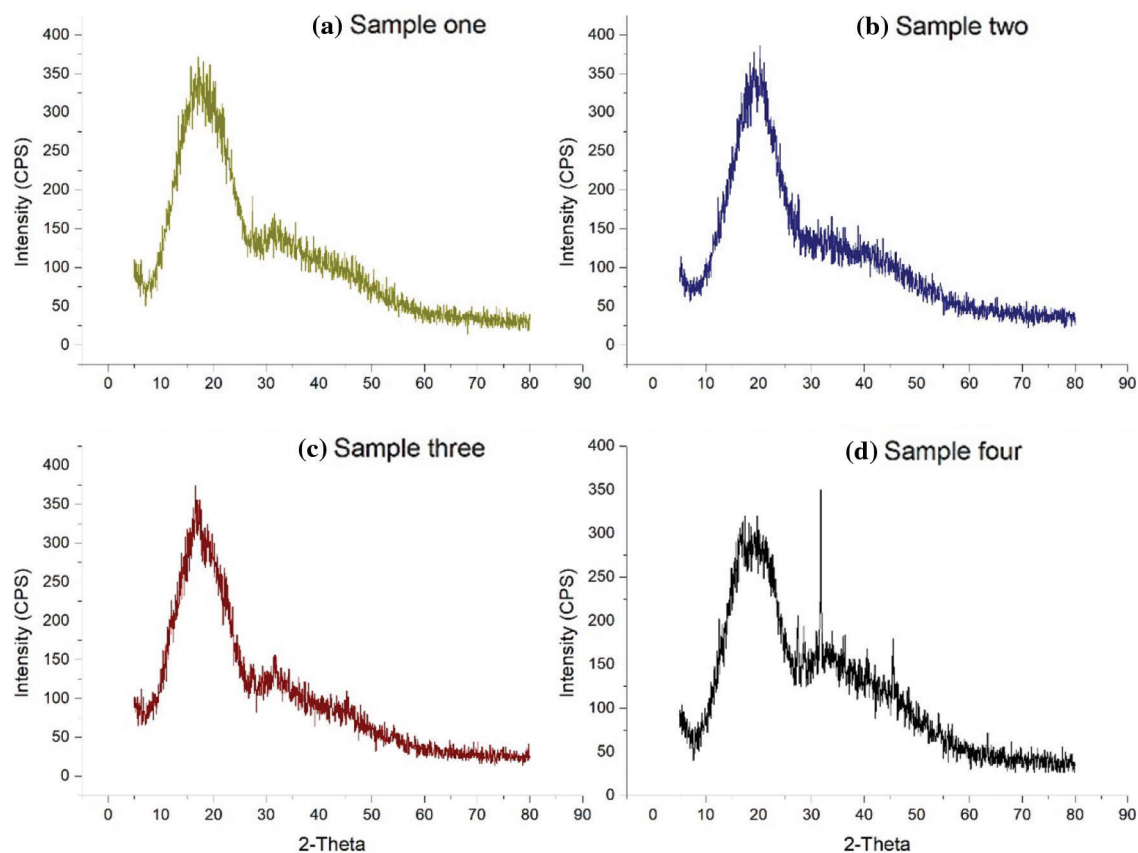


**Figure 9:** Shows the XRD spectrum of four test samples obtained from Shimadzu XRD-6000 X-ray Diffractometer at the Materials Research Department of the Ministry of Science and Technology in Baghdad, Iraq. (a) polylactic acids (sample one), (b) the XRD spectrum of polylactic acids injected with soybean oil resin (sample two), (c) immerse polylactic acids (sample three), (d) immerse polylactic acids injected with soybean oil resin (sample four)

**Table 6:** XRD spectral data for different samples

	Strongest three peaks No.	2-Theta (deg)	d ( $\text{\AA}^0$ )	Intensity	FWHM (deg)
Sample 1					
	1	17.1198	5.17524	46	0
	2	16.5709	5.34541	44	0
	3	15.7728	5.61405	44	0.48760
Sample 2					
	1	20.3618	4.35797	63	0
	2	19.1156	4.63917	59	0
	3	20.9601	4.23490	52	0

(Continued)

<b>Table 6 (continued)</b>					
	Strongest three peaks No.	2-Theta (deg)	d (Å <sup>0</sup> )	Intensity	FWHM (deg)
Sample 3					
	1	16.6208	5.32948	70	1.47140
	2	17.3693	5.10146	55	0.98580
	3	19.1187	4.63843	41	0.89380
Sample 4					
	1	31.8315	2.80902	103	0.28940
	2	17.0200	5.20536	62	0
	3	16.5709	5.34541	62	0

#### 4 Conclusion

This work aims to investigate the morphology of various samples and propose a novel approach that combines traditional FDM printing with a plant-based resin (soybean resin) to generate a biocompatible tissue engineering scaffold and assess the bioactivity of materials used to construct the scaffolds. Traditionally, soybean resin was only printed using a stereolithography (SLA) three-dimensional printer, which uses heating and laser, which can degrade and affect the morphology and structure of the materials.

In conclusion, when we compare non-immersed and immersed PLA samples (samples one and three), we notice small degradation on the surface of the immersed sample and a layer of ions attached to the surface, primarily sodium and chloride.

Furthermore, an immerse sample of PLA and soybean oil resin (sample four) demonstrates that the resin layer attracts more elements to precipitate than the PLA part. When immerse samples (samples three and four) are compared, we notice the formation of tricalcium phosphate on the surface of sample four injected with soybean resin; This sample also attracts a greater number of elements on its surface.

**Acknowledgement:** The authors thank Department of biomedical engineering AL-Nahrain University Baghdad/Iraq, Tehran University Iran, Materials Research Department of the Ministry of Science and Technology Baghdad/Iraq.

**Funding Statement:** The authors received no specific funding for this study.

**Conflicts of Interest:** The authors declare that they have no conflicts of interest to report regarding the present study.

#### Reference

1. Adriana Martel Estrada, S., Olivas Armendáriz, I., Torres García, A., Francisco Hernández Paz, J., Alejandra Rodríguez González, C. (2017). Evaluation of in vitro bioactivity of 45s5 bioactive glass/poly lactic acid scaffolds produced by 3D printing. *International Journal of Composite Materials*, 7(5), 144–149. DOI 10.5923/j.comaterials.20170705.03.
2. Aki, D., Ulag, S., Unal, S., Sengor, M., Ekren, N. et al. (2020). 3D printing of PVA/hexagonal boron nitride/ bacterial cellulose composite scaffolds for bone tissue engineering. *Materials and Design*, 196, 109094. DOI 10.1016/j.matdes.2020.109094.
3. Alam, F., Varadarajan, K. M., Kumar, S. (2020). 3D printed polylactic acid nanocomposite scaffolds for tissue engineering applications. *Polymer Testing*, 81, 106203. DOI 10.1016/j.polymertesting.2019.106203.

4. Ambekar, R. S., Kandasubramanian, B. (2019). Progress in the advancement of porous biopolymer scaffold: Tissue engineering application. *Industrial and Engineering Chemistry Research*, 58(16), 6163–6194. DOI 10.1021/acs.iecr.8b05334.
5. Arany, P., Róka, E., Mollet, L., Coleman, A. W., Perret, F. et al. (2019). Fused deposition modeling 3D printing: Test platforms for evaluating post-fabrication chemical modifications and in-vitro biological properties. *Pharmaceutics*, 11(6), 277. DOI 10.3390/pharmaceutics11060277.
6. Babilotte, J., Guduric, V., Le Nihouannen, D., Naveau, A., Fricain, J. C. et al. (2019). 3D printed polymer–Mineral composite biomaterials for bone tissue engineering: Fabrication and characterization. *Journal of Biomedical Materials Research Part B: Applied Biomaterials*, 107(8), 2579–2595. DOI 10.1002/jbm.b.34348.
7. Baino, F., Yamaguchi, S. (2020). The use of simulated body fluid (SBF) for assessing materials bioactivity in the context of tissue engineering: Review and challenges. *Biomimetics*, 5(4), 1–19. DOI 10.3390/biomimetics5040057.
8. Bardot, M., Schulz, M. D. (2020). Biodegradable Poly (Lactic Acid) Nanocomposites for Fused Deposition Modeling 3D Printing. *Nanomaterials*, 10(12), 2567. DOI 10.3390/nano10122567.
9. Choi, W. J., Hwang, K. S., Kwon, H. J., Lee, C., Kim, C. H. et al. (2020). Rapid development of dual porous poly (lactic acid) foam using fused deposition modeling (FDM) 3D printing for medical scaffold application. *Materials Science and Engineering C*, 110, 110693. DOI 10.1016/j.msec.2020.110693.
10. Choksi, N., Desai, H. (2017). Synthesis of biodegradable polylactic acid polymer by using lactic acid monomer. *International Journal of Applied Chemistry*, 13(2), 377–384.
11. Corrales, L. P., Esteves, M. L., Vick, J. E. (2014). Scaffold design for bone regeneration. *Journal of Nanoscience and Nanotechnology*, 14(1), 15–56. DOI 10.1166/jnn.2014.9127.
12. Cox, S. C., Thornby, J. A., Gibbons, G. J., Williams, M. A., Mallick, K. K. (2015). 3D printing of porous hydroxyapatite scaffolds intended for use in bone tissue engineering applications. *Materials Science and Engineering C*, 47, 237–247. DOI 10.1016/j.msec.2014.11.024.
13. Deng, F., Liu, L., Li, Z., Liu, J. (2021). 3D printed ti6al4v bone scaffolds with different pore structure effects on bone ingrowth. *Journal of Biological Engineering*, 15(1), 1–13. DOI 10.1186/s13036-021-00255-8.
14. dos Santos Silva, A., Rodrigues, B. V. M., Oliveira, F. C., Carvalho, J. O., de Vasconcellos, L. M. R. et al. (2019). Characterization and *in vitro* and *in vivo* assessment of poly(butylene adipate-co-terephthalate)/nano-hydroxyapatite composites as scaffolds for bone tissue engineering. *Journal of Polymer Research*, 26(2), 53. DOI 10.1007/s10965-019-1706-8.
15. Ghassemi, T., Shahroodi, A., Ebrahimzadeh, M. H., Mousavian, A., Movaffagh, J. et al. (2018). Current concepts in scaffolding for bone tissue engineering. *Archives of Bone and Joint Surgery*, 6(2), 90–99. DOI 10.22038/abjs.2018.26340.1713.
16. Gregor, A., Filová, E., Novák, M., Kronek, J., Chlup, H. et al. (2017). Designing of PLA scaffolds for bone tissue replacement fabricated by ordinary commercial 3D printer. *Journal of Biological Engineering*, 11(1), 1–21. DOI 10.1186/s13036-017-0074-3.
17. Guo, Z. (2017). *Porous scaffolds prepared using selective enzymatic degradation for tissue engineering*, pp. 34063–34070. DOI 10.1039/c7ra03574h.
18. Hassanajili, S., Karami-Pour, A., Oryan, A., Talaei-Khozani, T. (2019). Preparation and characterization of PLA/PCL/HA composite scaffolds using indirect 3D printing for bone tissue engineering. *Materials Science and Engineering C*, 104, 109960. DOI 10.1016/j.msec.2019.109960.
19. Ilhan, E., Ulag, S., Sahin, A., Yilmaz, B. K., Ekren, N. et al. (2021). Fabrication of tissue-engineered tympanic membrane patches using 3D-printing technology. *Journal of the Mechanical Behavior of Biomedical Materials*, 114, 104219. DOI 10.1016/j.jmbbm.2020.104219.
20. Jammalamadaka, U., Tappa, K. (2018). Recent advances in biomaterials for 3D printing and tissue engineering. *Journal of Functional Biomaterials*, 9(1), 22. DOI 10.3390/jfb9010022.
21. Janmohammadi, M., Nourbakhsh, M. S. (2020). Recent advances on 3D printing in hard and soft tissue engineering. *International Journal of Polymeric Materials and Polymeric Biomaterials*, 69(7), 449–466. DOI 10.1080/00914037.2019.1581196.

22. Ji, K., Wang, Y., Wei, Q., Zhang, K., Jiang, A. et al. (2018). Application of 3D printing technology in bone tissue engineering. *Bio-Design and Manufacturing*, 1(3), 203–210. DOI 10.1007/s42242-018-0021-2.
23. Khaledi, S., Jafari, S., Hamidi, S., Molavi, O., Davaran, S. (2020). Preparation and characterization of PLGA-PEG-PLGA polymeric nanoparticles for co-delivery of 5-fluorouracil and chrysin. *Journal of Biomaterials Science, Polymer Edition*, 31(9), 1107–1126. DOI 10.1080/09205063.2020.1743946.
24. Kondiah, P. P. D., Choonara, Y. E., Kondiah, P. J., Marimuthu, T., du Toit, L. C. et al. (2020). Recent progress in 3D-printed polymeric scaffolds for bone tissue engineering. In: *Advanced 3D-printed systems and nanosystems for drug delivery and tissue engineering*, pp. 59–81. DOI 10.1016/b978-0-12-818471-4.00003-0.
25. Koons, G. L., Diba, M., Mikos, A. G. (2020). Materials design for bone-tissue engineering. *Nature Reviews Materials*, 5(8), 584–603. DOI 10.1038/s41578-020-0204-2.
26. Li, Y., Chen, S. K., Li, L., Qin, L., Wang, X. L. et al. (2015). Bone defect animal models for testing efficacy of bone substitute biomaterials. *Journal of Orthopaedic Translation*, 3(3), 95–104. DOI 10.1016/j.jot.2015.05.002.
27. Luo, Y., Li, Y., Qin, X., Wa, Q. (2018). 3D printing of concentrated alginate/gelatin scaffolds with homogeneous nano apatite coating for bone tissue engineering. *Materials and Design*, 146, 12–19. DOI 10.1016/j.matdes.2018.03.002.
28. Merolli, A., Nicolais, L., Ambrosio, L., Santin, M. (2010). A degradable soybean-based biomaterial used effectively as a bone filler *in vivo* in a rabbit. *Biomedical Materials*, 5(1), 015008. DOI 10.1088/1748-6041/5/1/015008.
29. Nandi, S. K., Fielding, G., Banerjee, D., Bandyopadhyay, A., Bose, S. (2018). 3D-printed  $\beta$ -TCP bone tissue engineering scaffolds: Effects of chemistry on *in vivo* biological properties in a rabbit tibia model. *Journal of Materials Research*, 33(14), 1939–1947. DOI 10.1557/jmr.2018.233.
30. Nandiyanto, A. B. D., Oktiani, R., Ragadhita, R. (2019). How to read and interpret ftir spectroscopy of organic material. *Indonesian Journal of Science and Technology*, 4(1), 97–118. DOI 10.17509/ijost.v4i1.15806.
31. Ou, K. L., Hou, P. J., Huang, B. H., Chou, H. H., Yang, T. et al. (2020). Bone healing and regeneration potential in rabbit cortical defects using an innovative bioceramic bone graft substitute. *Applied Sciences*, 10(18), 6239. DOI 10.3390/AP10186239.
32. Pecci, R., Baiguera, S., Ioppolo, P., Bedini, R., Del Gaudio, C. (2020). 3D printed scaffolds with random microarchitecture for bone tissue engineering applications: Manufacturing and characterization. *Journal of the Mechanical Behavior of Biomedical Materials*, 103, 103583. DOI 10.1016/j.jmbbm.2019.103583.
33. Qu, H., Fu, H., Han, Z., Sun, Y. (2019). Biomaterials for bone tissue engineering scaffolds: A review. *RSC Advances*, 9(45), 26252–26262. DOI 10.1039/c9ra05214c.
34. Reis, D., Biscaia, S., Seabra, I. J., Veloso, A., Morouço, P. (2019). Fabrication of poly (Glycerol sebacate)-poly ( $\epsilon$ -caprolactone) extrusion-based scaffolds for cartilage regeneration. *Applied Mechanics and Materials*, 890, 268–274. DOI 10.4028/www.scientific.net/amm.890.268.
35. Rojas-Martínez, L. E., Flores-Hernández, C. G., López-Marín, L. M., Martínez-Hernández, A. L., Thorat, S. B. et al. (2020). 3D printing of PLA composites scaffolds reinforced with keratin and chitosan: Effect of geometry and structure. *European Polymer Journal*, 141, 1–10. DOI 10.1016/j.eurpolymj.2020.110088.
36. Rosenzweig, D. H., Carelli, E., Steffen, T., Jarzem, P. (2015). *3D-printed ABS and PLA scaffolds for cartilage and nucleus pulposus tissue regeneration*, pp. 15118–15135. DOI 10.3390/ijms160715118.
37. Stratakis, E. (2018). Novel biomaterials for tissue engineering 2018. *International Journal of Molecular Sciences*, 19(12), 19–22. DOI 10.3390/ijms19123960.
38. Tang, X., Qin, Y., Xu, X., Guo, D., Ye, W. et al. (2019). Fabrication and *in vitro* evaluation of 3D printed porous polyetherimide scaffolds for bone tissue engineering. *BioMed Research International*, 2019, 1–8. DOI 10.1155/2019/2076138.
39. Tariq, U., Haider, Z., Chaudhary, K., Hussain, R., Ali, J. (2018). Calcium to phosphate ratio measurements in calcium phosphates using LIBS. *Journal of Physics: Conference Series*, 1027(1), 012015. DOI 10.1088/1742-6596/1027/1/012015.
40. Buj-Corral, I., Bagheri, A., Petit-Rojo, O. (2018). 3D printing of porous scaffolds with controlled porosity and pore size values. *Materials*, 11(9), 1532. DOI 10.3390/ma11091532.

41. Wan, M., Liu, S., Huang, D., Qu, Y., Hu, Y. et al. (2021). Biocompatible heterogeneous bone incorporated with polymeric biocomposites for human bone repair by 3D printing technology. *Journal of Applied Polymer Science*, 138(13), 1–13. DOI 10.1002/app.50114.
42. Wang, C., Huang, W., Zhou, Y., He, L., He, Z. et al. (2020). 3D printing of bone tissue engineering scaffolds. *Bioactive Materials*, 5(1), 82–91. DOI 10.1016/j.bioactmat.2020.01.004.
43. Wen, Y., Xun, S., Haoye, M., Baichuan, S., Peng, C. et al. (2017). 3D printed porous ceramic scaffolds for bone tissue engineering: A review. *Biomaterials Science*, 5(9), 1690–1698. DOI 10.1039/c7bm00315c.
44. Wickramasinghe, S., Do, T., Tran, P. (2020). FDM-based 3D printing of polymer and associated composite: A review on mechanical properties, defects and treatments. *Polymers*, 12(7), 1529. DOI 10.3390/polym12071529.
45. Yao, Q., Wei, B., Guo, Y., Jin, C., Du, X. et al. (2015). Design, construction and mechanical testing of digital 3D anatomical data-based PCL–HA bone tissue engineering scaffold. *Journal of Materials Science: Materials in Medicine*, 26(1), 51. DOI 10.1007/s10856-014-5360-8.
46. Yu, Y., Hua, S., Yang, M., Fu, Z., Teng, S. et al. (2016). Fabrication and characterization of electrospinning/3D printing bone tissue engineering scaffold. *RSC Advances*, 6(112), 110557–110565. DOI 10.1039/C6RA17718B.
47. Zheng, X., Lee, S. K., Chun, O. K. (2016). Soy isoflavones and osteoporotic bone loss: A review with an emphasis on modulation of bone remodeling. *Journal of Medicinal Food*, 19(1), 1–14. DOI 10.1089/jmf.2015.0045.
48. Harahap, I. A. (2021). Probiotics and isoflavones as a promising therapeutic for calcium status and bone health: A narrative review. *Foods*, 10(11), 2685. DOI 10.3390/foods10112685.
49. Nayeem, F., Chen, N. W., Nagamani, M., Anderson, K. E., Lu, L. J. W. (2019). Daidzein and genistein have differential effects in decreasing whole body bone mineral density but had no effect on hip and spine density in premenopausal women: A 2-year randomized, double-blind, placebo-controlled study. *Nutrition Research*, 68, 70–81. DOI 10.1016/j.nutres.2019.06.007.
50. Chu, Z., Zhao, T., Li, L., Fan, J., Qin, Y. (2017). Characterization of antimicrobial poly (lactic acid)/nano-composite films with silver and zinc oxide nanoparticles. *Materials*, 10(6), 659. DOI 10.3390/ma10060659.
51. Kien, P. T., Quan, T. N., Tuyet Anh, L. H. (2021). Coating characteristic of hydroxyapatite on titanium substrates via hydrothermal treatment. *Coatings*, 11(10), 1–11. DOI 10.3390/coatings11101226.